

Electronic Supplementary Information

Light-responsive hybrid material based on luminescent core-shell quantum dots and steroidal organogels

L. C. Schmidt,^a V. C. Edelsztein,^b C. C. Spagnuolo,^c P. H. Di Chenna^{b*} and R. E. Galian^{d*}

^a. INFIQC-CONICET, Departamento de Química Orgánica, Facultad de Ciencias Químicas, Universidad Nacional de Córdoba, 5000 Córdoba, Argentina.

^b. UMYMFOR-CONICET, Departamento de Química Orgánica, Facultad de Ciencias Exactas y Naturales, Universidad de Buenos Aires, Ciudad Universitaria, C1428EGA, Buenos Aires, Argentina. E-mail: dichenna@qo.fcen.uba.ar

^c. CIHIDECAR-CONICET, Departamento de Química Orgánica, Facultad de Ciencias Exactas y Naturales, Universidad de Buenos Aires, Ciudad Universitaria, C1428EGA, Buenos Aires, Argentina.

^d. ICMOL, Universidad de Valencia, Catedrático José Beltrán 2, 46980, Paterna, Valencia, España. E-mail: raquel.galian@uv.es

Table of contents

Table S1 Optical properties of the synthesized quantum dots.	S3
Figure S1: Absorption and emission spectra of CT and CA.	S4
Figure S2: Absorption and emission spectra of CST and CSA.	S5
Figure S3: High resolution transmission electron microscopy of quantum dots: a) CT, b) CA, C) CST and d) CSA. Scale bar 20 nm.	S6
Table S2 Photophysical properties of the QD-OG1 hybrids	S7
Figure S4 a) Fluorescence emission spectra and b) fluorescence kinetic trace of CST in <i>n</i> -hexane, CST+ OG1 (0.1 wt. % in <i>n</i> -hexane) and c) CST-OG1.	S8
Table S3 Photophysical properties of CST at increasing concentration of OG1.	S9
Figure S5 Fluorescence lifetime of CST in solution.	S10
Figure S6 Ratio of radiative and non-radiative rate constant values of CST in the presence of increasing concentrations of OG1.	S11
Figure S7. ^1H NMR (500 MHz) CDCl_3 (OG1)	S12
Figure S8. ^1H NMR (500 MHz) CDCl_3 (CST- OG1)	S12
Figure S9. ^{31}P NMR (500 MHz, CDCl_3) spectra of TOPO and TOPO+OG1	S13
Figure S10 FT- FT-IR spectra of CST, OG1 and OG1-CST mixture.	S14
Figure S11 FT- IR spectra of OG1, TOPO and TOPO+OG1 mixture.	S15
Figure S12: Variation of CST-OG1 fluorescence with the temperature.	S16
Figure S13: Effect of small amount of a) acetone (50 μl), b) water (20 μl) and c) <i>n</i> -hexane (150 μl) on the luminescence properties of the CST-OG1	S17
Figure S14 Fluorescence quenching of CST in the presence of DAE	S18
Figure S15 TEM images of CST-OG1 hybrid in the presence of DAE before and after photoswitching experiment.	S19
Figure S16 UV-visible absorption spectra of TOPO OG1 and DAE.	S20

Table S1. Optical properties of the synthesized quantum dots.

NPs	λ_{ab} , (nm)	λ_{em} , (nm)	FWHM (nm)	Φ^a	Diameter (nm)	
					UV ^b	HRTEM
CT	519	529.0	28	9.3	2.55	2.6
CA	515	523.5	29	3.4	2.50	2.6
CST	519	532.6	27	55.0	2.55	4.0
CSA	513	529.4	28	46.4	2.48	4.7

^a Calculated using fluorescein as standard fluorophore, excitation at 465 nm.

^b Calculated using the maximum in the UV-visible spectra ¹

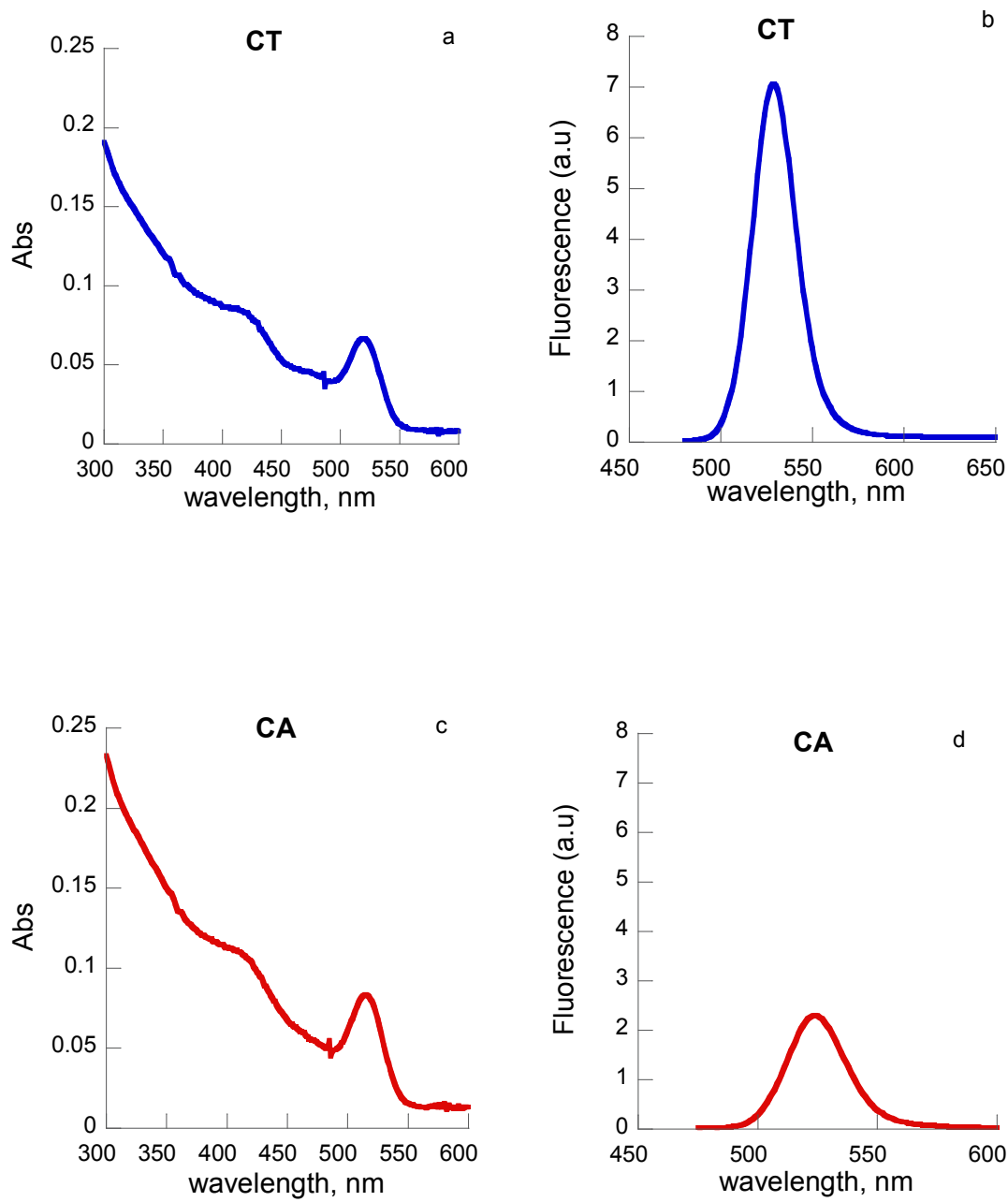


Figure S1: Absorption and emission spectra ($\lambda_{\text{exc}} = 465 \text{ nm}$) of CT (a, b) and CA (c, d) with a concentration of $1 \cdot 10^{-6} \text{ M}$ in toluene.

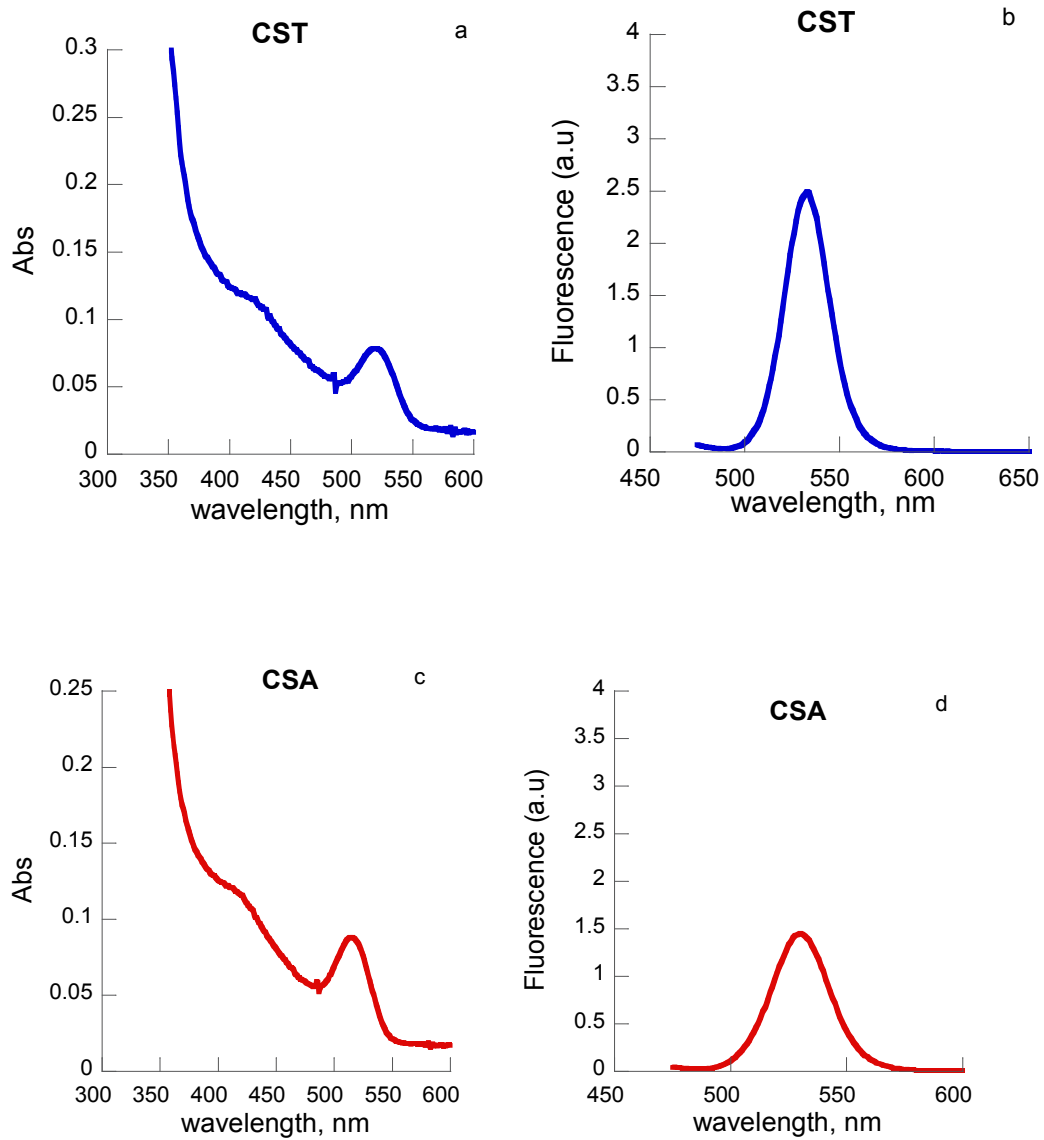


Figure S2: Absorption and emission spectra ($\lambda_{\text{exc}} = 465 \text{ nm}$) of CST (a, b) and CSA (c, d) with a concentration of $1.1 \cdot 10^{-6} \text{ M}$ in toluene.

HTEM images of QDs

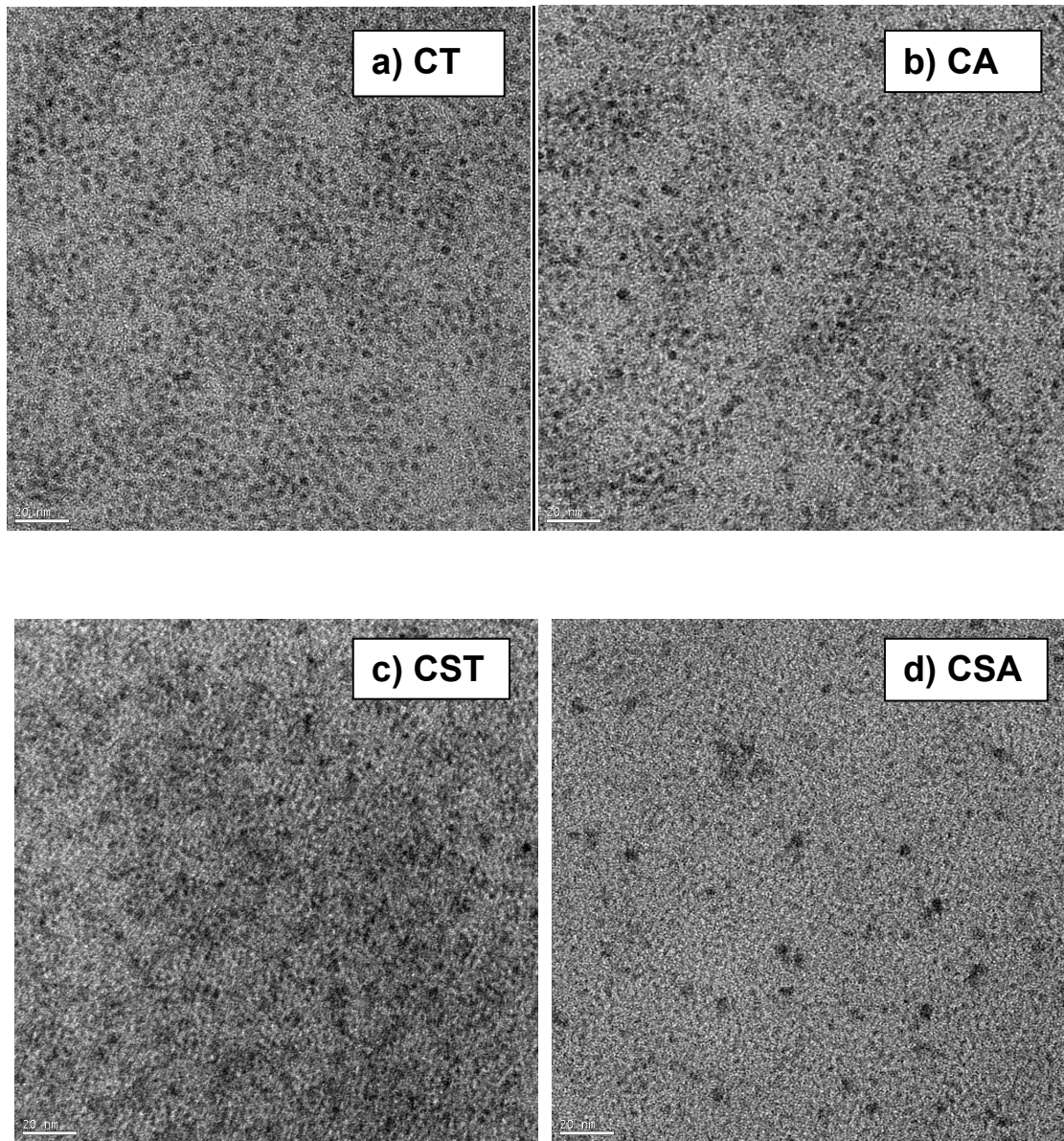


Figure S3: High resolution transmission electron microscopy of quantum dots: a) CT, b) CA, C) CST and d) CSA. Scale bar 20 nm.

Table S2 Photophysical properties of the QD-OG1 hybrids

QD or QD-OG1	λ_{em} , (nm)	Φ^{a}	τ_{av} (ns)	K_r , 10^6 s^{-1}	K_{nr} , 10^6 s^{-1}
CT	529.0	9.1	-	-	-
CT-OG1	529.0	0	-	-	-
CA	523.5	3.4	160.9	0.21	6.0
CA-OG1	523.5	0.9	29.1	0.33	34.0
CST	532.6	55.0	69.6	7.90	6.46
CST-OG1	532.6	25.7	45.2	5.75	16.4
CSA	529.4	46.4	152.3	3.02	3.5
CSA-OG1	529.4	11.7	60.9	1.92	14.5

^a Calculated using fluorescein as standard fluorophore, excitation at 465 nm.

Values of k_r and k_{nr} in table S2 were obtained according to the fluorescence lifetime equation S1 combined with equation S2 (Lakowicz, Principles of Fluorescence Spectroscopy, 3rd edition). The average lifetime τ_{av} obtained for the multiexponential luminescence decay was used in both equations.

$$\tau_{\text{av}} = \frac{1}{(k_r + k_{nr})} \quad \text{Equation S1}$$

$$\phi = \frac{k_r}{k_r + k_{nr}} = \tau_{\text{av}} \cdot k_r \quad \text{Equation S2}$$

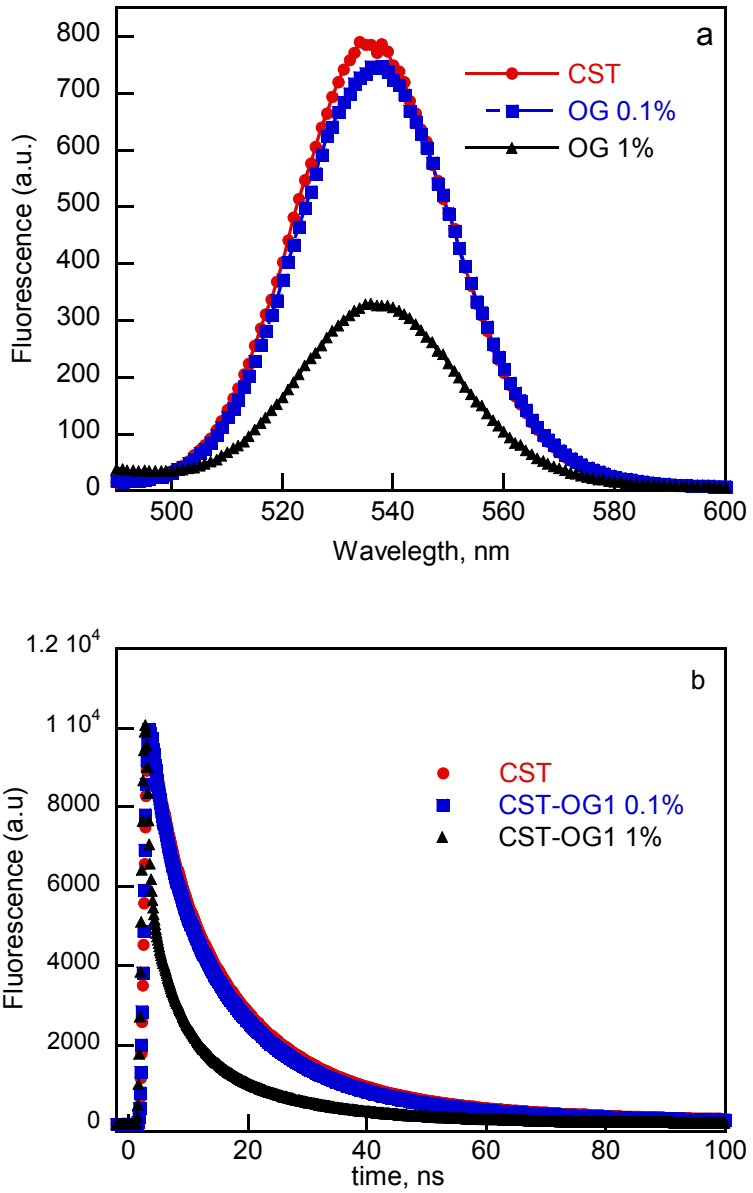


Figure S4 a) Fluorescence emission spectra and b) fluorescence kinetic trace of **CST** in *n*-hexane, **CST+ OG1** (0.1 wt.% in *n*-hexane) and **CST-OG1** (1 wt.% in *n*-hexane). $\lambda_{\text{exc}} = 457 \text{ nm}$

Table S3 Photophysical properties of CST at increasing concentration of OG1 in chloroform.

OG (% w/v)	τ_{av} (ns)	Φ_F	Area	$k_r \cdot 10^6 s^{-1}$	$K_{nr} \cdot 10^6 s^{-1}$
0	58.1	0.5501	28675.51	9.47	7.74
0.5	53.6	0.4549	23713.04	8.49	10.17
1	52.62	0.3622	18881.79	6.89	12.12
1.5	49.59	0.3090	16109.48	6.23	13.93
2	49.02	0.2865	14935.65	5.84	14.55
2.5	50.05	0.2630	13712.6	5.25	14.73
3	47.2	0.2423	12630.43	5.13	16.05

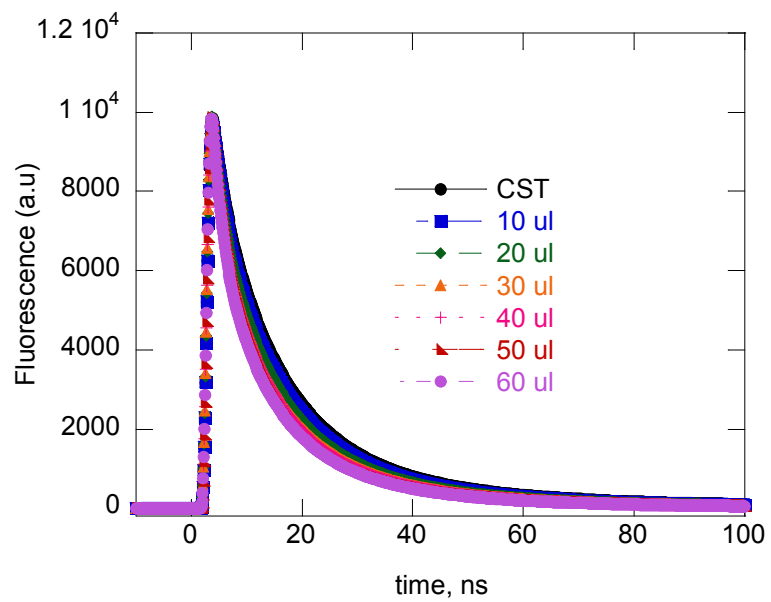


Figure S5 Fluorescence lifetime of **CST** in solution, at increasing concentration of **OG1** in chloroform. $\lambda_{\text{exc}} = 457 \text{ nm}$

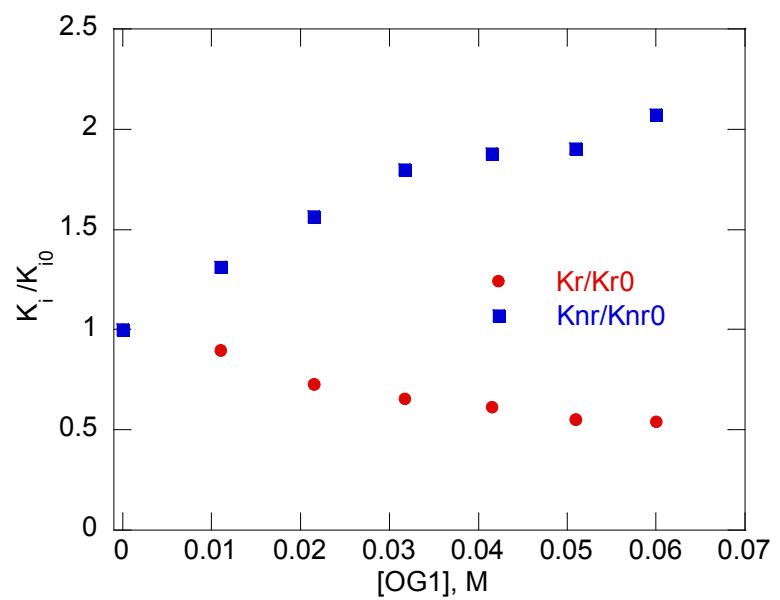


Figure S6 Ratio of radiative and non-radiative rate constant values of CST in the presence of increasing concentrations of OG1 in chloroform.

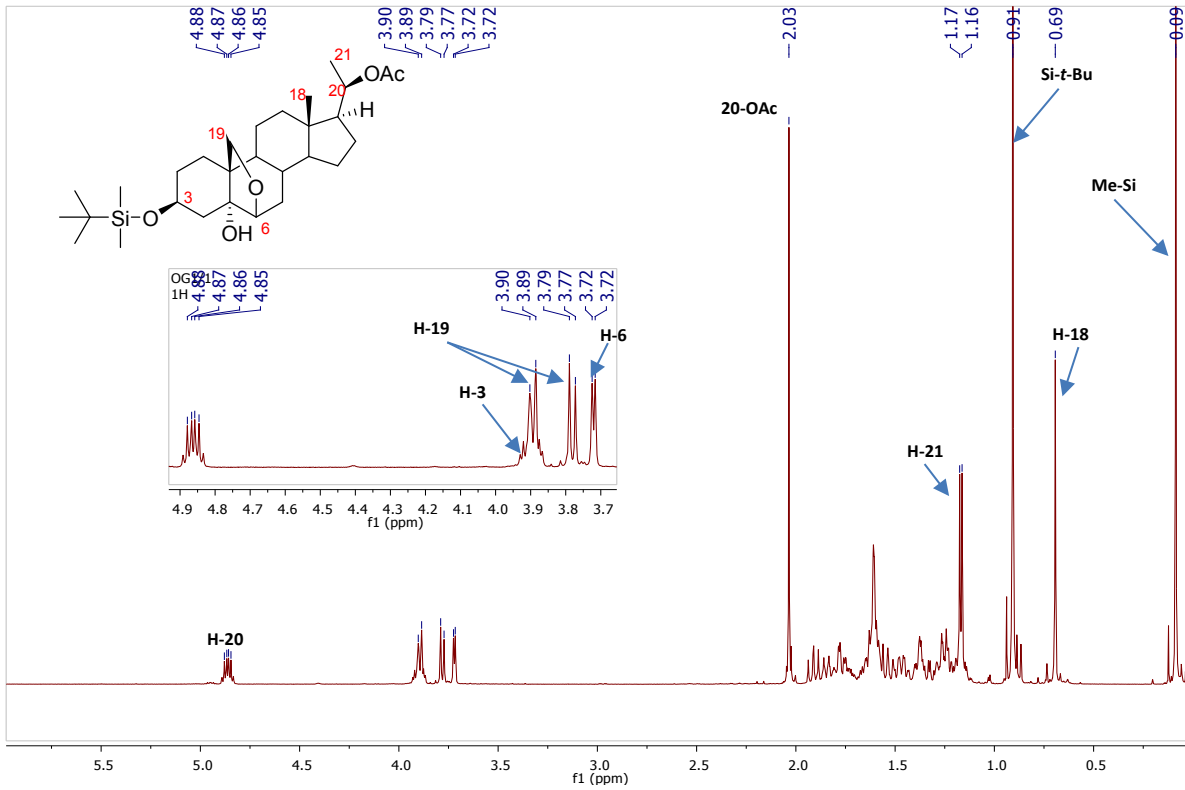


Figure S7. ^1H NMR (500 MHz) CDCl_3 (**OG1**)

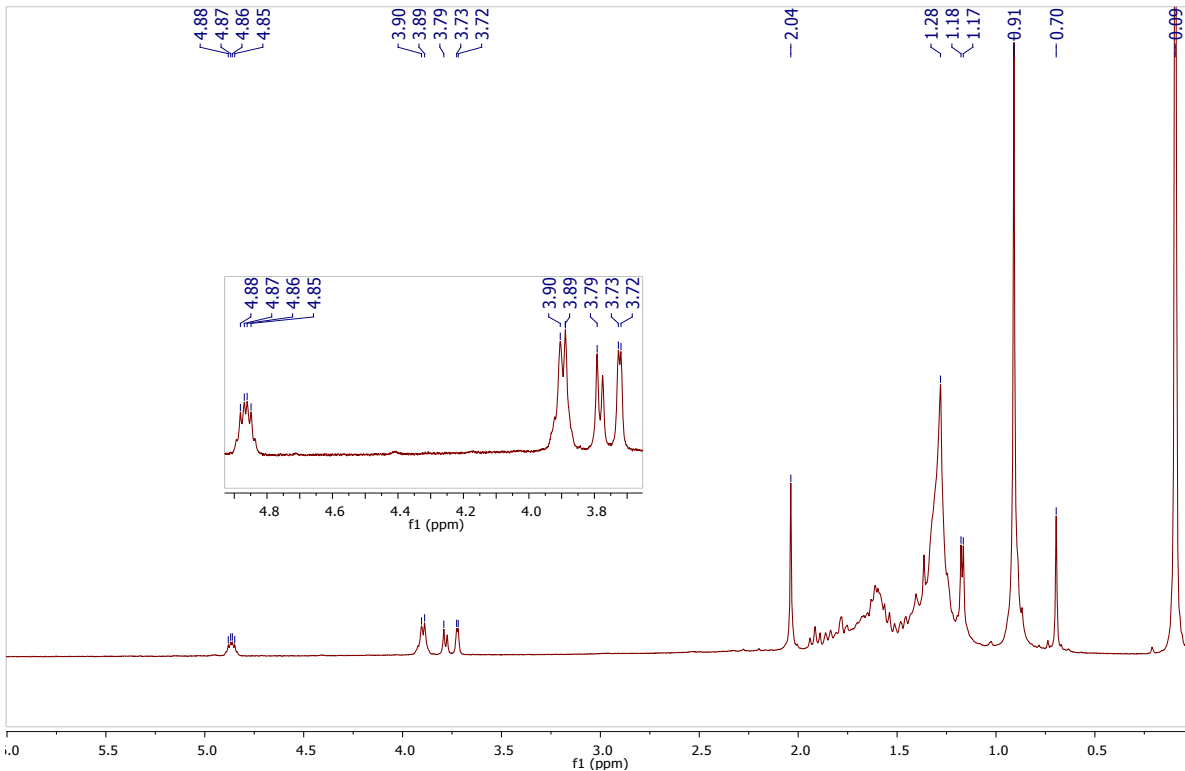


Figure S8. ^1H NMR (500 MHz) CDCl_3 **CST- OG1**

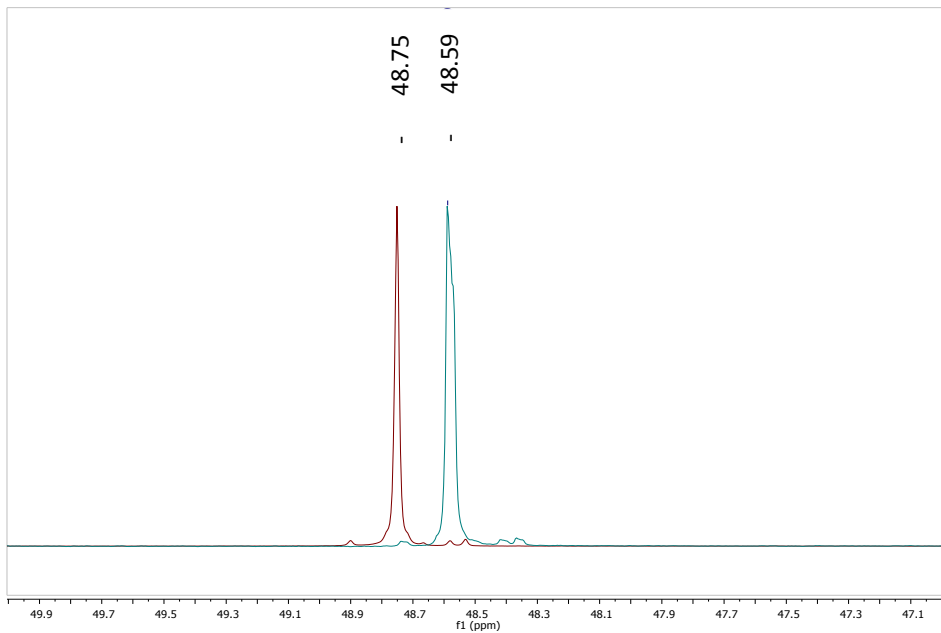
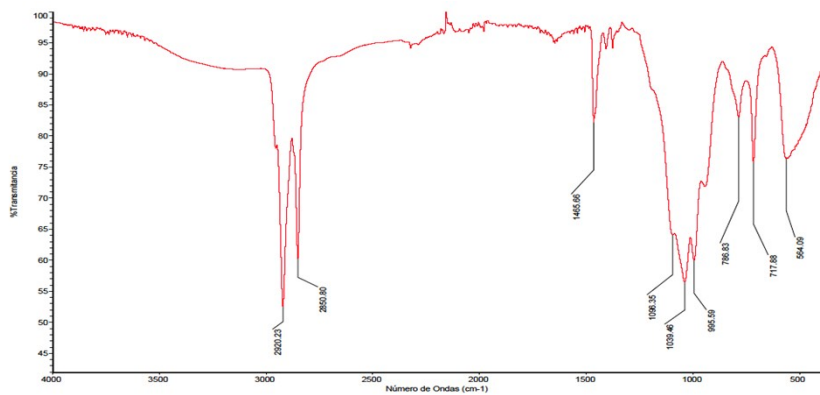
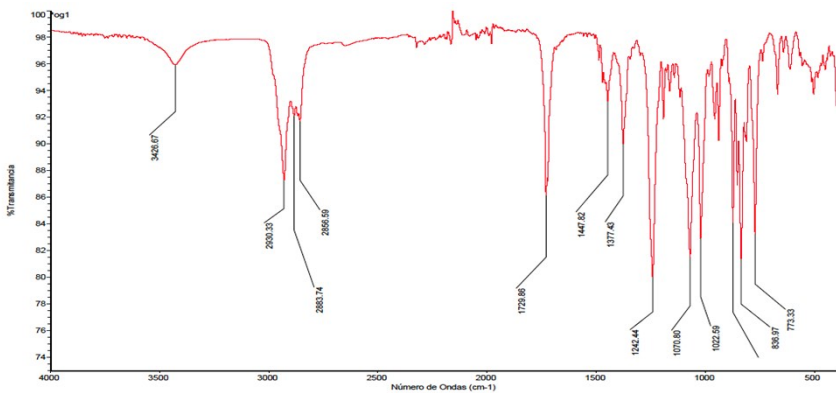


Figure S9. ^{31}P NMR (202.5 MHz, CDCl_3) superimposed spectra, in green TOPO (20 mM) FWHM: 6.3Hz and brown TOPO (20 mM) + **OG1** (20 mM) FWHM: 3.2 Hz.

a)



b)



c)

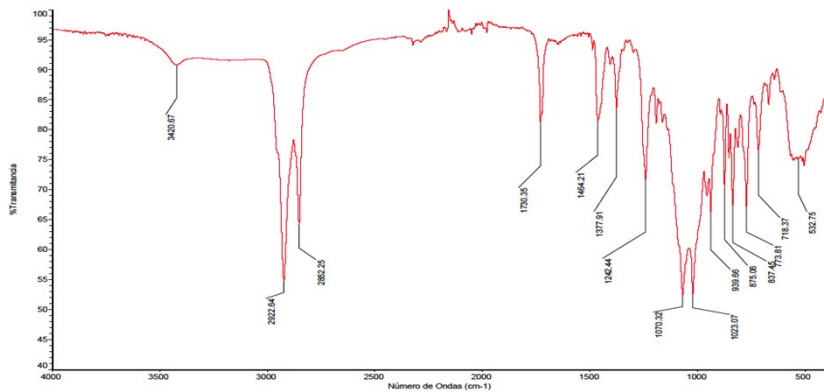


Figure S10. FT-IR spectra of a) CST b) OG1 and c) OG1-CST.

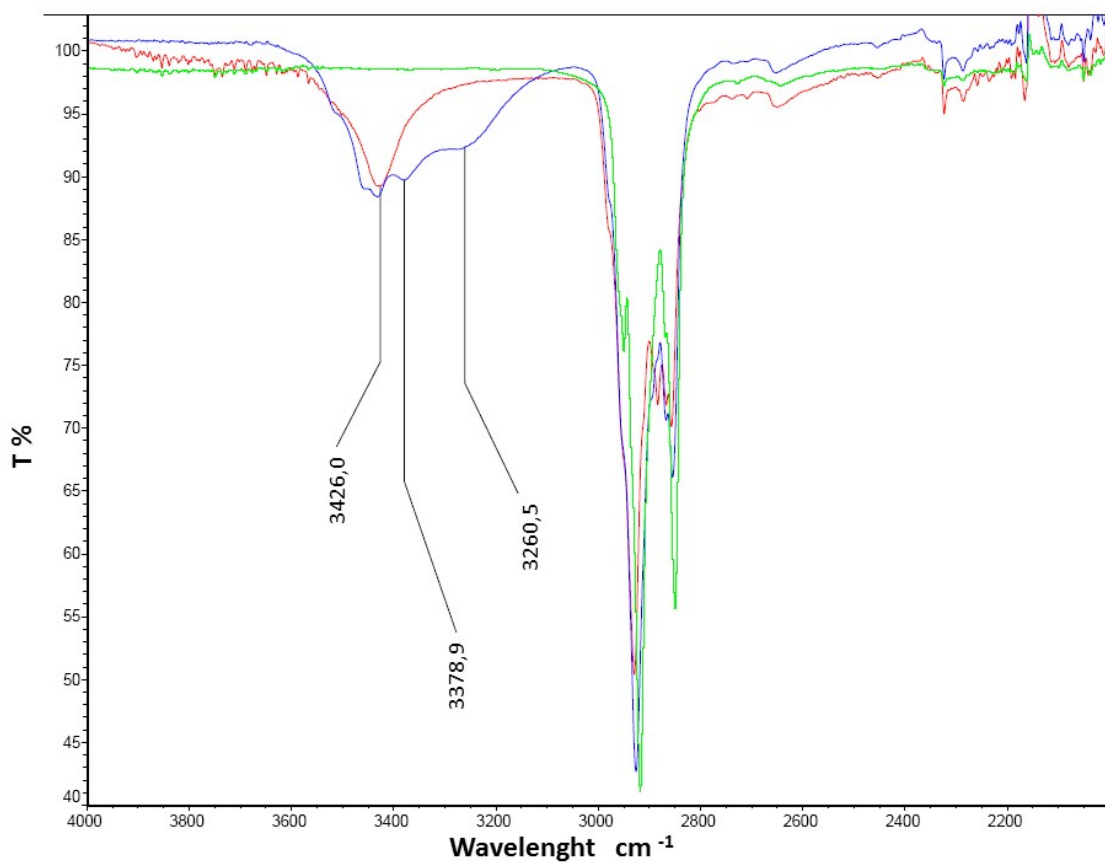


Figure S11. FT- IR spectra of **OG1** (red), **TOPO** (green) and **TOPO+OG1** mixture (blue).

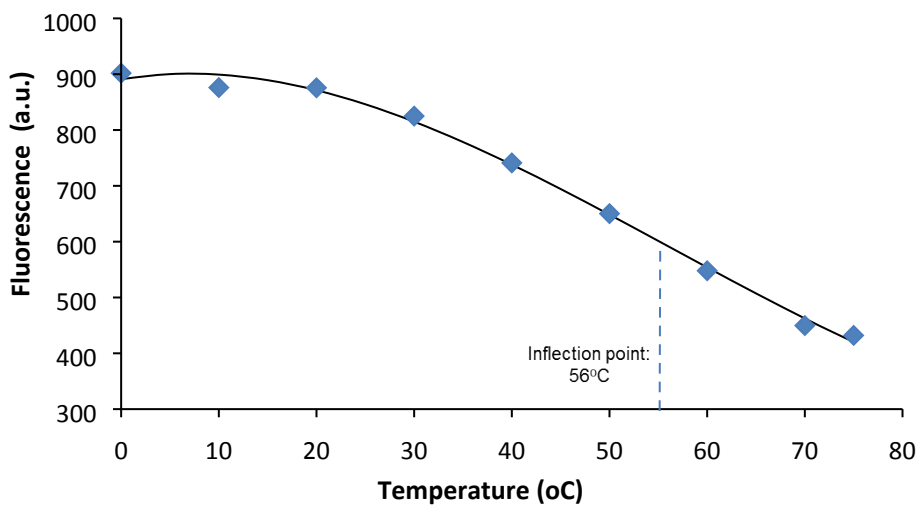


Figure S12: Variation of the CST-OG1 fluorescence with the temperature Maximum values for the fluorescence emission spectra of QD-CST in solution and in the organogel from *n*-hexane; $\lambda_{\text{exc}} = 400$ nm. Temperature was raised from 0 to 75°C. Concentrations in the OG1-CST hybrid: OG1 1 wt. %, QD-CST 1.14 μ M. The Tg value could be measured at the inflection point ($T_g = 56$ °C).

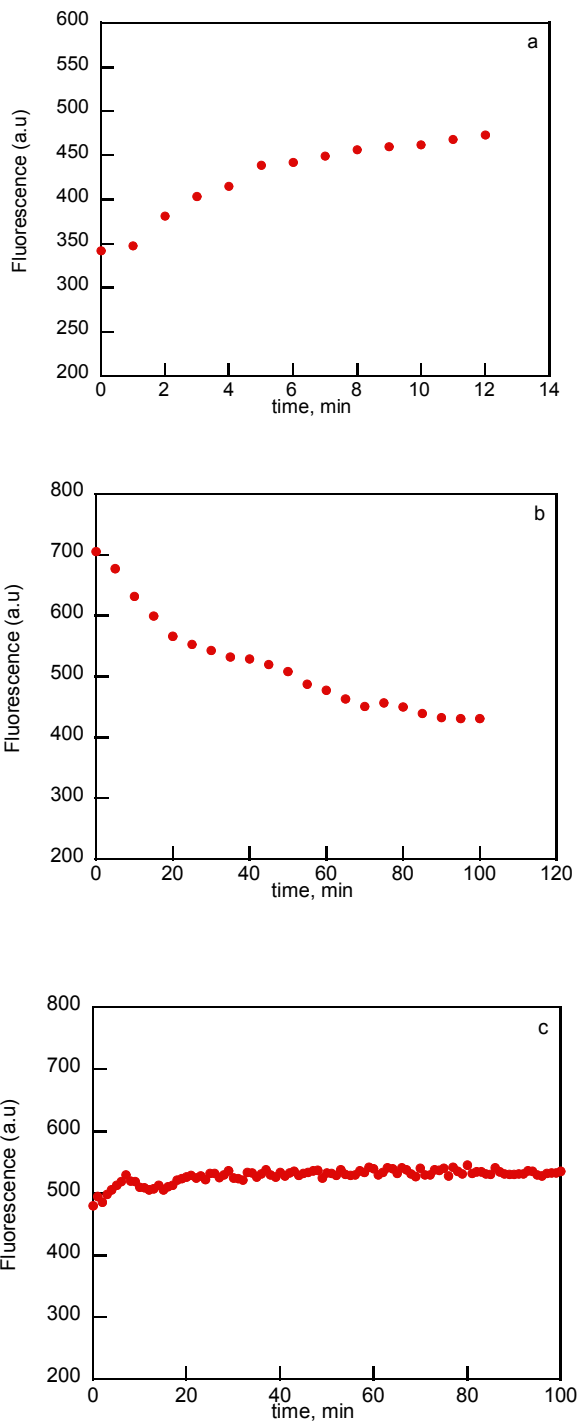


Figure S13: Effect of small amount of a) acetone (50 µL), b) water (20 µL) and c) *n*-hexane (150 µL) on the luminescence properties of the CST-OG1.

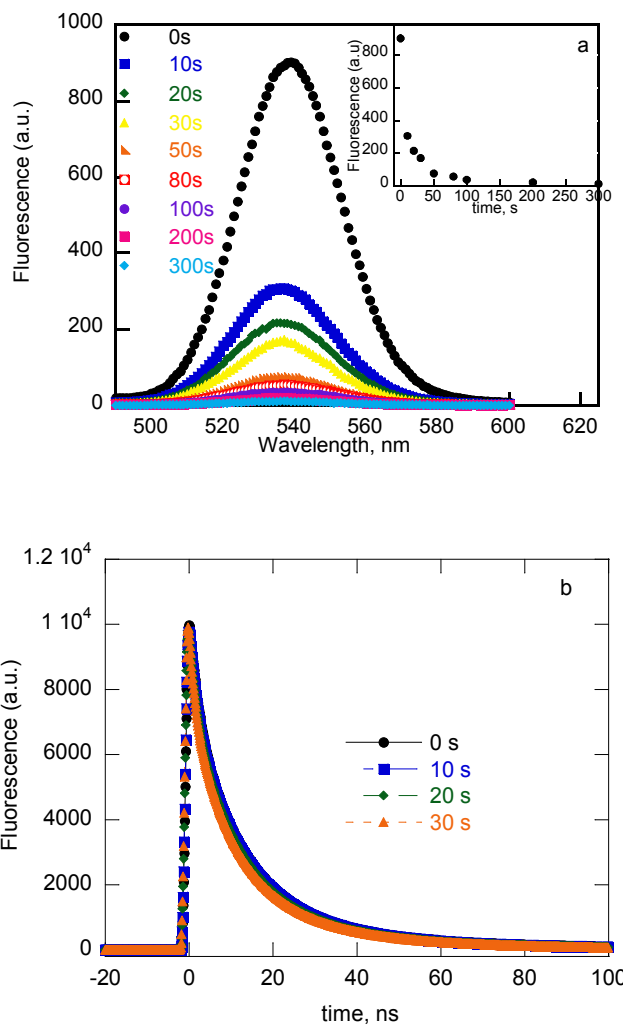


Figure S14 Fluorescence quenching of CST in the presence of DAE (2.5 mM) at different irradiation time with UV light (340 nm), quenching efficiency = 95%. a) Fluorescence spectra, inset fluorescence intensity at 537 nm vs. irradiation times; and b) Fluorescence kinetic traces.

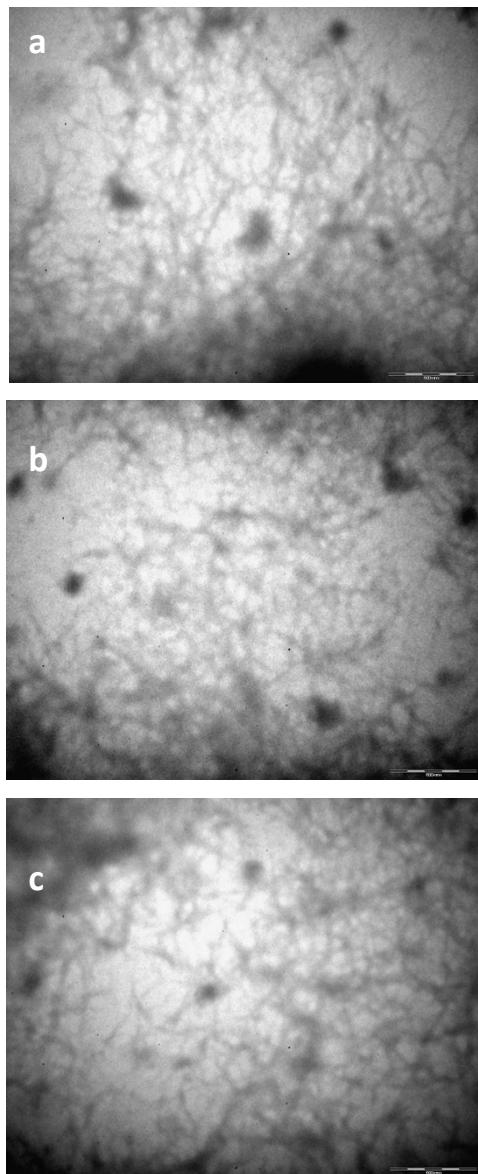


Figure S15 TEM images of CST-OG1 hybrid in the presence of DAE a) before and b) after photoswitching experiment. c) Morphology control of a Xerogel of OG1 after irradiation (conditions of the photoswitching experiment).

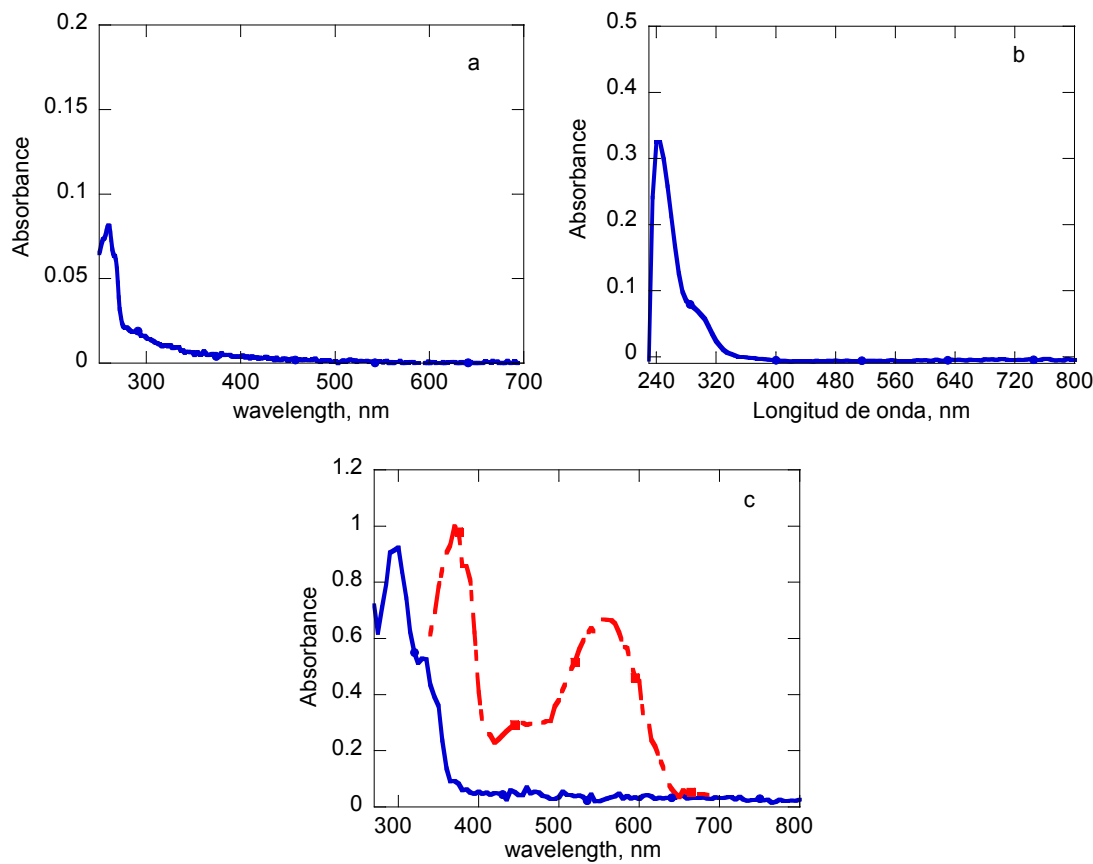


Figure S16 UV-visible absorption spectra of a) TOPO in *n*-hexane, b) OG1 in dichloromethane and c) OPEN form of DAE (blue line) and CLOSE form of DAE (red line) in dichloromethane.

1. W. W. Yu, L. Qu, W. Guo and X. Peng, *Chemistry of Materials*, 2003, **15**, 2854-2860.